Irregular Wave Forces on Monopile Foundations. Effect af Full Nonlinearity and Bed Slope

Schløer, Signe; Bredmose, Henrik; Bingham, Harry B.

Published in:
Proceedings of the ASME 30th 2011 International Conference on Ocean, Offshore and Arctic Engineering

Publication date:
2011

Document Version
Publisher's PDF, also known as Version of record

Proceedings of the ASME 30th 2011 International Conference on Ocean, Offshore and Arctic Engineering
OMAE2011
June 19-24, 2011, Rotterdam, The Netherlands

OMAE2011-49709

IRREGULAR WAVE FORCES ON MONOPILE FOUNDATIONS. EFFECT OF FULL NONLINEARITY AND BED SLOPE.

Signe Schløer
DTU Mechanical Engineering
DK-2800 Kgs. Lyngby
Denmark
Email: sigs@mek.dtu.dk

Henrik Bredmose
DTU Mechanical Engineering
DK-2800 Kgs. Lyngby
Denmark
Email: hbr@mek.dtu.dk

Harry B. Bingham
DTU Mechanical Engineering
DK-2800 Kgs. Lyngby
Denmark
Email: hbb@mek.dtu.dk

ABSTRACT

Forces on a monopile from a nonlinear irregular unidirectional wave model are investigated. Two seabed profiles of different slopes are considered. Morison's equation is used to investigate the forcing from fully nonlinear irregular waves and to compare the results with those obtained from linear wave theory and with stream function wave theory. The latter of these theories is only valid on a flat bed. The three predictions of wave forces are compared and the influence of the bed slope is investigated. Force-profiles of two selected waves from the irregular wave train are further compared with the corresponding force-profiles from stream function theory.

The results suggest that the nonlinear irregular waves give rise to larger extreme wave forces than those predicted by linear theory and that a steeper bed slope increases the wave forces both for linear and nonlinear waves. It is further found that stream function theory in some cases underestimate the wave forces acting on the monopile.

INTRODUCTION

The offshore wind industry is increasing tremendously in these years. There is therefore a focus on making the design of the wind turbine and foundation as cost effective as possible. The wind farms are being moved further offshore where the wave loads become larger relative to the wind loads and therefore more important in the design. In this context it is beneficial to have a hydrodynamic model which describes the waves and the associated loads as accurately as possible.

Waves are a stochastic process. Hence, to capture all the effects from the waves an irregular wave theory should be used. At the same time offshore wind farms are often placed in intermediate or shallow water where wave nonlinearity is important. This however is usually ignored and instead linear/second-order waves are applied for irregular waves and stream function wave theory is used to describe the extreme waves although this theory is restricted to regular waves on a flat bed.

For this reason it is important to investigate the significance of nonlinearity for irregular waves both in the determination of the extreme loads where the irregular nonlinear waves can become more steep than waves from nonlinear regular wave theory and in the determination of fatigue loads where nonlinear waves will transfer energy to higher frequencies which can be close to the wind turbines eigenfrequency.

Agarwal and Manuel (2009) used an integrated wind-wave response simulation analysis program in order to compare the loads of linear and second-order nonlinear irregular waves. They concluded that it is important to consider nonlinear wave loads in the design. Gravesen et al. (2003) used a fully nonlinear Boussinesq wave model to study the wave forces but did not compare the loads with linear wave loads. This motivates an investigation into the effects of nonlinearity on the loads from irregular waves on wind turbine foundations. Further, as full wave nonlinearity is usually only taken into account through stream function wave theory for regular waves on constant depth, an assessment of the effect of local bed slope is relevant.

In the present paper the effects of nonlinearity and bed slope for the design of a monopile foundation are investigated. Two examples of nonlinear irregular force distributions over depth are further compared with stream function wave forces, in order to get an idea of the error associated with the application of stream function waves in the design of extreme wave loads.

The fully nonlinear potential flow wave model of Engsig-Karup et al. (2008) (see also Bingham and Zhang (2007)) is used to calculate time series of irregular waves.

The monopile is placed in a water depth of 20 m on a sloping bed. This water depth is representative for many of the wind farms which are built these years (e.g. Anholt Denmark, Beaufort The Netherlands and Borkum Riffgrund Germany).

Two seabed profiles with average slopes of 1:25 and 1:100 are compared. The slope of 1:25 is quite steep, yet it is relevant to investigate the effect of this seabed slope since small slopes (e.g. 1:100) are difficult to achieve in the laboratory as it requires a long wave flume.

The investigation shows that the nonlinear irregular waves differ from the linear irregular waves and that both nonlinearity and a steeper bed slope increase the wave loads. It is further found that the wave forces due to irregular nonlinear waves are larger than that predicted by stream function wave theory.

MODEL SETUP

The fully nonlinear potential wave model of Engsig-Karup et al. (2008) is used to compute unidirectional irregular waves. The model is based on a finite difference flexible–order solver for the potential flow approximation for non-overturning waves.

The horizontal wave force per meter length of the pile with diameter D = 5m are calculated using Morison's equation

$$f(z,t) = \frac{1}{2}\rho C_D D u(z,t)|u(z,t)| + \rho C_M A a(z,t) \tag{1}$$

Here $\rho = 1025\,\mathrm{m}^2/\mathrm{s}$ is the density of the water, A the cross sectional areal of the pile, $C_D = 1.0$ and $C_M = 2.0$ the drag- and inertia coefficient, respectively, $u(z,t)$ the horizontal particle velocity and $a(z,t)$ the horizontal particle acceleration.

The inline force and overturning moment can then be found as

$$F(t) = \int_{z=-h}^{z=\eta} f(z,t)dz \tag{2}$$

$$M(t) = \int_{z=-h}^{z=\eta} f(z,t)z dz \tag{3}$$

The surface elevation η and vertical- and horizontal particle velocities, v and u, are provided by the numerical model on nine points between the sea bed and the free surface, associated with the numerical grid applied. The vertical position of these points, Z, varies with time and the horizontal particle acceleration in a single point must therefore be evaluated through the chain rule as

$$a(z,t) = \frac{\partial u}{\partial t} = \frac{du}{dt} - \frac{\partial u}{\partial Z}\frac{\partial Z}{\partial t} \tag{4}$$

The term $\frac{\partial u}{\partial Z}$ is also provided by the numerical model, while the time derivatives $\frac{du}{dt}$ and $\frac{\partial Z}{\partial t}$ were calculated as post-processing using the midpoint rule on a 5 point stencil which is accurate to fourth order.

In order to study the effect of nonlinearity, the nonlinear irregular waves were compared to linear irregular waves. As linear wave theory is only valid up to mean water level, Wheeler stretching was used in order to stretch the irregular linear velocity and acceleration from the mean water level up to the real surface elevation. Although Wheeler stretching only is an alternative linear approximation of the velocity field it is widely considered to give a more realistic description of the wave kinematic between sea water level and surface elevation.

Two seabed profiles with different slopes are considered to investigate if the associated change in wave propagation affects the wave loads. The profiles are described as

$$h(x) = h_0 - \frac{1}{2}(h_0 - h_1)(1 + z(x)) \tag{5}$$

$$z(x) = \tanh\left(\sin\left(\frac{\frac{\pi}{2}x}{1-x^2}\right)\right) \tag{6}$$

At the left boundary the water depth is $h_0 = 50\,\mathrm{m}$ and at the right boundary $h_1 = 17\,\mathrm{m}$. The first profile has a rather steep slope with a maximum of 1:25 and is referred to as the 1:25-profile in the following. The other case has a more mild slope with a maximum of 1:100 and is referred to as the 1:100-profile. The comparison of the waves takes place at a water depth of 20 m. At this point the slopes have a value of 1:36 and 1:139, respectively. The two profiles are shown in figure 1.

The physical characteristics of the wave climate used for the computations equals a two year wave return period taken from the Metocean report from Anholt Offshore Wind Farm, Kattegat, Denmark (Grode (2009)) which is planned to be build in 2012-2013. The significant wave height is $H_s = 2.8\,\mathrm{m}$ and the peak period is $T_p = 6.8\,\mathrm{s}$. For this relatively mild condition, no wave breaking occur in the computations, and full validation of the wave model is therefore ensured. Computations of more extreme wave climates require the inclusion of a wave breaking model and is left as future work.

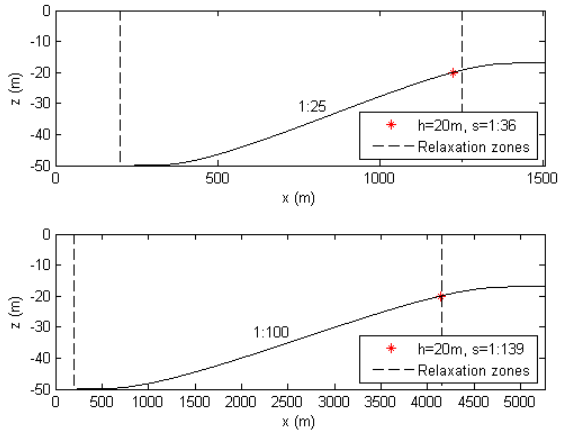

FIGURE 1: The two profiles, dashed line indicates the relaxation-zones and the red start where $h = 20\,\mathrm{m}$.

The first part of the computational domain is a relaxation zone where the waves are generated. The input wave is a linear wave time series described by a JONSWAP-spectrum. At the left boundary where the waves are generated the nondimensional wave number is $kh = 4.4$ at the spectral peak frequency. This justifies the approximation of linear wave theory for the offshore wave condition. At the end of the domain another relaxation zone is defined where the waves are damped out in order to avoid reflection. The relaxation zones are indicated in figure 1.

A consequence of using a fully nonlinear wave model is the development of numerical instabilities at high frequencies. A filter is therefore required which removes these high frequency instabilities. In these computations a 10th-order 13-point Savitzky-Golay smoothing filter is applied after every time step. The filter removes the energy at high frequencies close to the Nyqvist frequency but leaves the wave frequencies intact, cf. Engsig-Karup et al. (2008).

RESULTS

For both seabed profiles a linear and a fully nonlinear time series of the irregular waves were computed. In order to compare the time series, probability plots of surface elevation, inline force and overturning moment have been produced. In the time series. the largest positive and negative peak value between each zero-downcrossing were found. The positive and negative peaks were treated separately and sorted in increasing order. The percent point function was then calculated as

$$P(X_i) = \frac{i}{N} \tag{7}$$

where X_i is the i'th η,- F- or M-value sorted in increasing order and N the number of data.

1:25-profile

In the following the time series of the linear and nonlinear irregular waves for the 1:25-profile are compared. The time series of the surface elevation at $h = 20\,\mathrm{m}$ are shown in figure 2. The length of the time series is 8946 s. In the first part of the time series the surface elevation is zero because it takes some time for the wave train to propagate from $h = 50\,\mathrm{m}$ to $h = 20\,\mathrm{m}$. The numerical model further has to be run for some time before the waves are fully developed. For these present computations this "warm-up period" is approximately 302 s as indicated with two red lines in figure 2. The part of the time series which are compared starts at the ends of the "warm-up period" and end after 8142 s. This is indicated with black lines in figure 2.

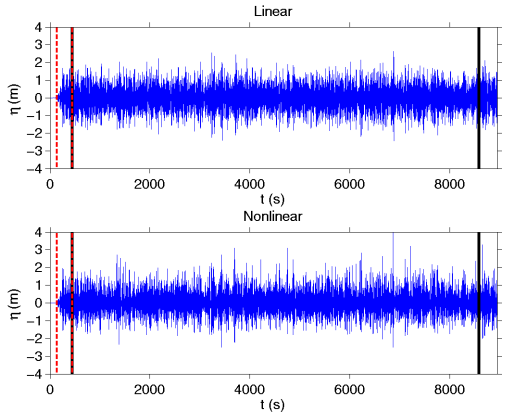

FIGURE 2: The linear and nonlinear time series for the 1:25-profie. The red dashed line indicates the "warm-up period". The black lines indicate the part of the time series which are compared.

The probability plots of η, F or M are seen in figure 3. The figure shows the probability of getting either η, F and M less than some certain value both for the linear and nonlinear irregular waves. The probability plot of the maximum crest- and trough surface elevations are shown in separate figures as is the case for the positive and negative peak forces and peak moments. For the negative surface elevations, peak forces and peak moments the sign is shifted, to allow direct comparison of the probabilities for the positive and negative values.

In the probability plot for the peak crest surface elevation $P(\eta)$, figure 3a top, it is clear that the nonlinear waves have

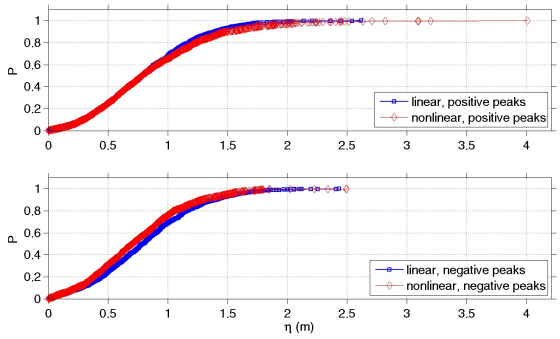

(a) Surface elevation

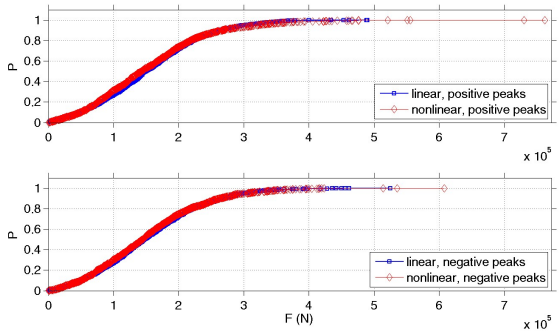

(b) Force

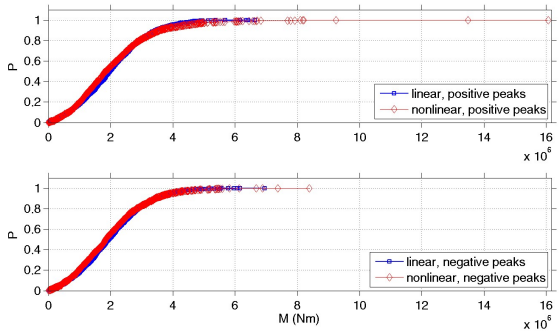

(c) Moment

FIGURE 3: Probability plots of surface elevation, inline force and overturning moment. Linear and nonlinear waves for the 1:25-profile.

larger crest values for the extreme waves. Seven nonlinear crest values are larger than the largest linear crest value and the probability of getting a crest value larger than $\eta = 1\,\text{m}$ is largest for the nonlinear wave. The probabilities of the peak trough values are compared in figure 3a, bottom. It is seen that the nonlinear waves have a less deep trough as the nonlinear probability curve lies above the linear probability curve in a large interval. Further, while the largest linear crest value is close to the largest linear trough value, the largest nonlinear crest value is significantly larger than the largest nonlinear trough value. These results are due to normal nonlinear effects: Nonlinear wave crests are higher and shorter and the wave troughs longer and less deep than for linear waves. For the force, figure 3b, the probability curves are comparable to the curves for the surface elevation. Five nonlinear positive peak forces are larger than the largest linear positive peak force and the probability of getting a positive peak force larger than $F = 0.3\,\text{MN}$ is largest for the nonlinear waves. The largest peak force in the negative probability curves, figure 3b bottom, is nonlinear. The negative and positive linear probability curves are quite similar while the largest nonlinear positive peak force is rather large compared with the largest nonlinear negative peak force. The similarity between the results for the free surface elevation and inline force illustrates the linear relation between those two quantities associated with an inertia-dominated structure where the dominant force contribution is due to the acceleration term in the Morison equation. The probability curves for the linear and nonlinear overturning moment is seen in figure 3c. The nonlinearity is more distinct in this figure compared with figure 3a and 3b. The probability of getting a positive moment larger than $M = 4\,\text{MNm}$ is largest for the nonlinear wave and 12 nonlinear positive peak moments are larger than the largest linear positive peak moment. The largest nonlinear positive peak moment is in addition more than twice the size of the largest linear positive peak moment. The largest negative and positive linear peak moment are quite equal as was the case for the probability curves of the linear surface elevation and linear force.

The results described above indicate that nonlinear irregular waves give rise to larger inline forces and overturning moments.

1:100-profile

The linear and nonlinear irregular time series for the 1:100-profile are now compared. The time series are seen in figure 4. The domain of the 1:100-profile is longer than the domain of the 1:25-profile and the surface elevation is therefore zero for a longer period. The "warm-up period" is again 302 s and the time series which are compared are 8142 s long.

The probability plots for the linear and nonlinear waves for the 1:100-profile are compared in figure 5. The nonlinear effects which were seen in the 1:25-profile are also seen here. The free surface elevation, inline force and overturning moment are significantly larger for the nonlinear waves especially for the positive peaks. The nonlinearity is again most distinct in the overturning moment where the largest positive nonlinear moment is twice the size of the largest linear positive moment.

The results from the 1:100-profile therefore verify the results from the 1:25-profile that the nonlinear irregular waves give rise to larger inline forces and overturning moments.

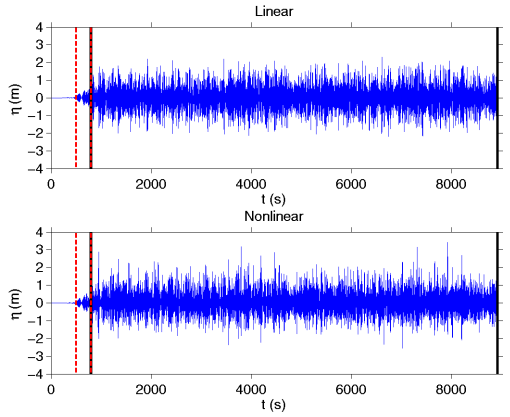

FIGURE 4: The linear and nonlinear time series for the 1:100-profile. The red dashed line indicates the "warm-up period". The black lines indicate the part of the time series which are compared.

Direct comparison for the two bed slopes

In order to compare the effects of nonlinearity on the two slopes we here compare the free surface elevations, peak force and overturning moment for the two slopes directly.

The probability plots of the nonlinear free surface elevations, peak forces and peak moments for the 1:25-profile and 1:100-profile are compared in figure 6. The curves are quite similar, except for the largest values where the 1:25-profile has the largest crest surface elevation, positive peak force and positive peak moments.

A comparison of the linear η, F and M for the two slopes is provided in figure 7. The 1:25-profile has approximately three to four values which are larger the largest value in the 1:100-profile both in probability plots of surface elevations, peak forces and peak moments. However, for the linear waves the difference between the two profiles is less distinct.

Thus both for the linear and nonlinear case, the extreme crest elevations, inline forces and overturning moments are largest for the steepest slope. Further, this effect is strongest for the nonlinear computation. This indicates that the nonlinearity enhances the increase in the loads due to the steeper slope.

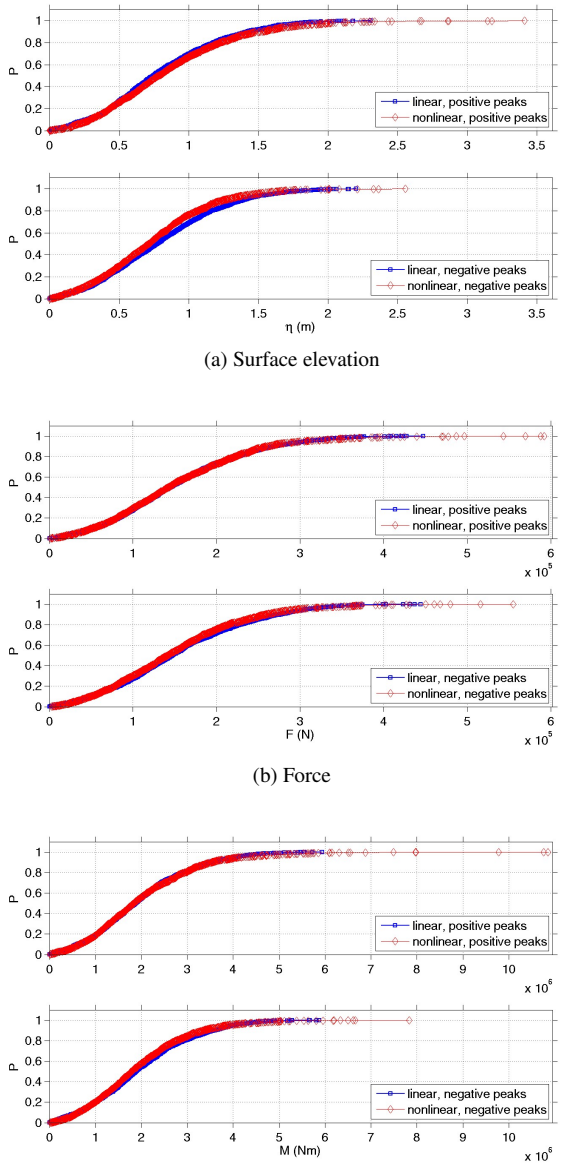

(a) Surface elevation

(b) Force

(c) Moment

FIGURE 5: Probability plots of surface elevation, inline force and overturning moment. Linear and nonlinear waves for the 1:100-profile.

Comparison between nonlinear irregular waves and stream function theory

We now compare the nonlinear irregular wave forces to stream function wave forces for selected waves on the two slopes. The stream function wave is calculated with basis in the wave height and wave period for the selected irregular waves. The wave height H is here defined as the distance between crest and trough between two zero-downcrossings. The wave period is the time between the two zero-downcrossings. For both the 1:25-profile and the 1:100-profile, the wave with the largest wave crest is chosen (figure 3a and 5a). For the 1:25-profile the corresponding wave height and wave period is $H = 5.14\,\text{m}$ and $T = 7.25\,\text{s}$. The irregular surface elevation and corresponding stream function surface elevation is compared in figure 8. The irregular wave

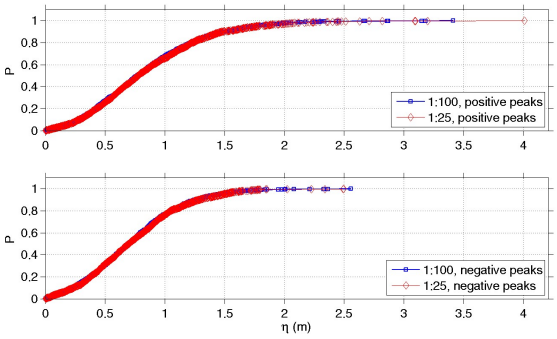

(a) Surface elevation

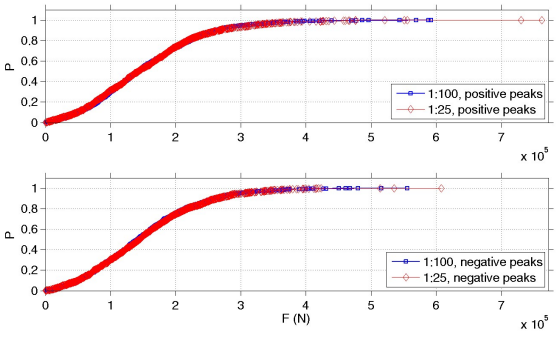

(b) Force

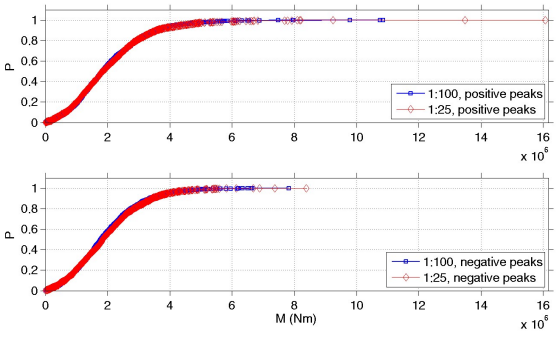

(c) Moment

FIGURE 6: Probability plots of surface elevation, inline force and overturning moment. Nonlinear waves for the 1:25-profile and 1:100-profile.

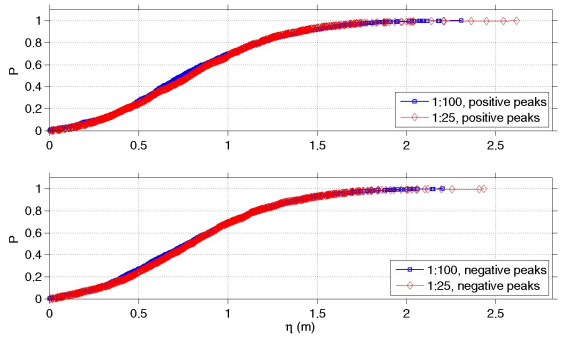

(a) Surface elevation

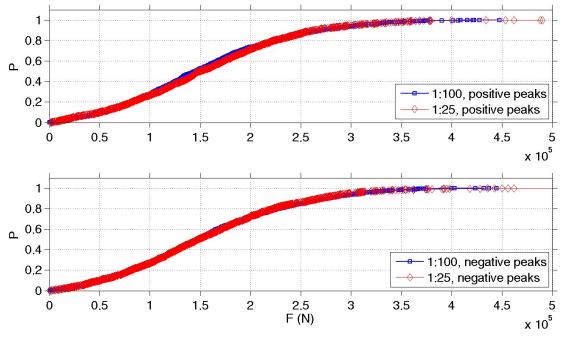

(b) Force

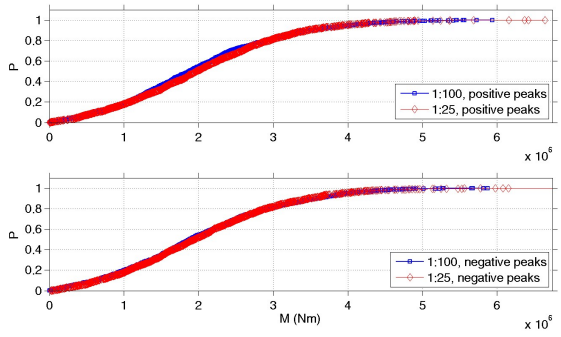

(c) Moment

FIGURE 7: Probability plots of surface elevation, inline force and overturning moment. Linear waves for the 1:25-profile and 1:100-profile.

is rather steep at the crest, and it has therefore been investigated how close it is to wave breaking. From the linear dispersion relation the length of the wave is estimated to $L = 76\,\text{m}$. The ratio between H and L is 0.07. On a horizontal bed wave breaking would not be expected before the ratio is approximately 0.14-0.15 and it is therefore assumed that the wave has not been subject to wave breaking. The irregular wave profile is seen to be lifted upwards vertically relative to the stream function wave. The difference in the shape of the waves is manifested in the vertical distribution of the wave force acting along the monopile, as shown in figure 9. The distribution of the wave force over the depth for the two waves is very different. At the surface the irregular force is

much larger than the stream function force. On the other hand the stream function force is largest from just below mean water level ($\eta \sim -2.5\,\mathrm{m}$) and down to the seabed. The irregular wave force is actually negative at the seabed.

For the 1:100-profile the wave which is compared has the wave height $H = 5.01\,\mathrm{m}$ and wave period $T = 6.00\,\mathrm{s}$. This irregular wave is compared with the corresponding stream function wave in figure 10. The irregular wave crest is again more steep and lifted more upwards compared with the stream function wave. The ratio between the wave length and wave height is for the irregular wave on a horizontal seabed 0.09. It is therefore again assumed that the irregular wave has not been subject to wave breaking. The vertical force distribution of the irregular wave and the stream function wave have been added to figure 9. In this case, the two predictions of wave force distribution are closer to each other. Still, however, the irregular wave force is three times larger at the surface elevation.

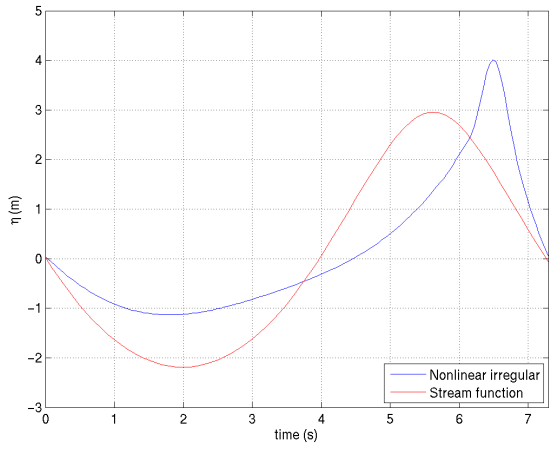

FIGURE 8: A nonlinear irregular wave for the 1:25-profile is compared with the corresponding stream function wave.

The inline force and overturning moment for the irregular and stream function waves of figure 9 are shown in table 1. The inline forces are for both profiles largest for the irregular waves. For the 1:25-profile the irregular wave force is 30 % larger than the corresponding stream function wave force. This effect is further exaggerated for the overturning moment, where for the 1:25-profile, the moment of the irregular wave is actually twise as large as that of the stream function wave. The large value of the overturning moment can be attributed to the steep rise of the irregular wave that leads to a large inline force and higher elevation of the irregular crest that leads to a larger moment arm.

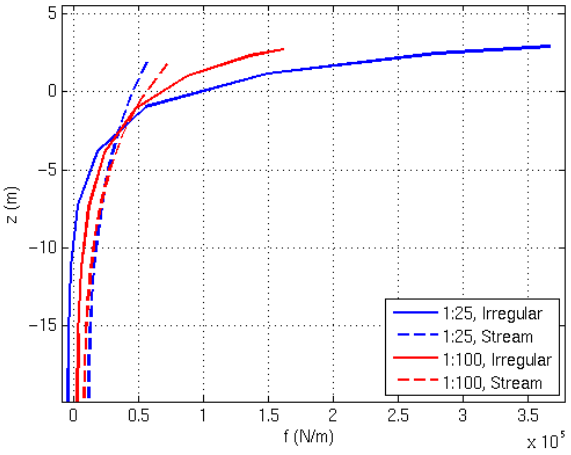

FIGURE 9: The forces due to the two nonlinear irregular waves and the corresponding stream function waves.

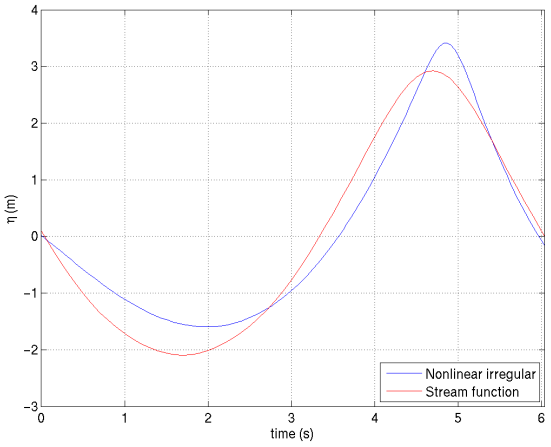

FIGURE 10: A nonlinear irregular wave for the 1:100-profile is compared with the corresponding stream function wave.

	$F_{T,irreg.}$	$F_{T,stream}$	$M_{T,irreg.}$	$M_{T,stream}$
1:25	0.76 MN	0.53 MN	16 MNm	7.6 MNm
1:100	0.60 MN	0.53 MN	10 MNm	8.1 MNm

TABLE 1: The inline force and the overturning moment for the waves shown in figure 8 and 10.

SUMMARY AND DISCUSSION

Forces on a monopile from fully nonlinear irregular unidirectional waves have been investigated. The surface elevation, inline force and overturning moment were compared with irregular linear waves and the effect from the seabed slope on the corresponding wave forces were studied.

When comparing the surface elevations a deviation between the linear and nonlinear irregular waves was found. The nonlinear waves had the largest crest values while the nonlinear trough values were smaller. This is due to normal nonlinear effects. The nonlinear effects were manifested in the inline force and overturning moment where the irregular nonlinear waves resulted in positive forces and positive moments which was significant larger than the irregular linear wave forces and moments. The difference in the forces and moments was made clear when two force-profiles of two selected irregular nonlinear waves were compared with the corresponding force-profiles from stream function theory. The irregular force-profiles was substantially larger at the free surface elevation resulting in larger irregular inline forces. The difference was even more pronounced in the overturning moments. The larger value of the overturning moment is due to the larger crest value of the nonlinear irregular wave which results in a larger moment arm. The results suggest that in the extreme wave load design, stream function theory in some cases underestimate the wave forces acting on the monopile.

The nonlinearity was most distinct for the 1:25-profile. Even for the linear waves there was a difference between the 1:25-profile and 1:100-profile. The linear extreme crest surface elevations, inline forces and overturning moments were largest in the 1:25-profile. For the nonlinear waves the nonlinearity enhanced this difference between the profiles. Hereby for the present wave climate, both nonlinearity and bed slope have been found to increase the wave loads.

It could be interesting to make the same computations with the same- and perhaps one more seabed profiles but with a stronger wave climate. The waves used in these investigations were relatively mild in order to avoid wave breaking. With a larger wave the nonlinear effects might be more significant. Such computations, however, requires the inclusion of a breaking model into the numerical code. This is currently work in progress.

Next step in this research project will be to combine the irregular fully nonlinear hydrodynamic model with an aeroelastic code. This will enable investigation of the balance between wave and wind contributions to the fatigue life time of offshore wind turbines.

REFERENCES

Agarwal, P. and L. Manuel (2009). Simulation of offshore wind turbine response for long-term extreme load prediction. *Engineering Structures 31*(10), 22362246.

Bingham, H. B. and H. Zhang (2007). On the accuracy of finite-difference solutions for nonlinear water waves. *Journal of Engineering Mathematics 58*(1-4), 211–228.

Engsig-Karup, A., H. Bingham, and O. Lindberg (2008, December). An efficient flexible-order model for 3D nonlinear water waves. *Journal of Computational Physics 228*(6), 2100–2118.

Gravesen, H., L. S. Larsen, H. B. Bingham, N. J. Tarp-Johansen, J. Pedersen, and P. Vølund (2003). Consequences of steep waves and large wave forces to offshore wind turbine design. In *European wind energy conference and exhibition*, Madrid (ES).

Grode, P. D. (2009). *Anholt Offshore Wind Farm, Metocean Data for Design and Operational Conditions*. Ramboll Oil and Gas, Teknikerbyen, 2830 Virum, Denmark. Metocean report prepared for the client Energinet.dk.

ACKNOWLEDGMENT

This research was carried out as part of the Statkraft Ocean Energy Research Program, sponsored by Statkraft (www.statkraft.no). This support is gratefully acknowledged. Assistant Professor Allan Engsig-Karup is thanked for providing access to the fully nonlinear wave model.